Geometric Deformable Model And Segmentation

Haiyan Wang

Dept. of Systems Sci. & Math
Washington University
St. Louis, MO 63130

Bijoy K. Ghosh

Dept. of Systems Sci. & Math
Washington University
St. Louis, MO 63130

Abstract

In this paper, we point out some problems associated with the existent geometric active contour models, and present a new geometric active contour model. This model can overcome some drawbacks in the previous geometric models. We implement the geometric active contour model using level set method. The efficacy of the proposed algorithm is demonstrated with experiments on synthetic images and medical images.

1 Introduction

Recovering the shapes of objects in 2D and 3D from various types of visual data is an important goal in computer vision and image processing. One way to achieve this goal is via model-based techniques. Snakes or active contour models introduced by Kass-Witkin-Terzopoulas[1] have been developed extensively among the model-based techniques. Recently, geometric active contour models were simultaneously proposed by Caselles et al.[2] and Malladi et al.[3] Those models are based on the curve evolution theory in differential geometry. The use of curvature driven flows and partial differential equation(PDE) in computer vision and image analysis has become a rising interest research topic in the past few years. Curve or surface evolution driven by a PDE has been studied from the theoretical standpoint[4-6] and from the viewpoint of numerical implementation[7-9] with the development of level set methods that can efficiently and robustly solve the PDEs. The applications of the curve or surface evolution theory to computer vision and image processing are based on moving curves or surfaces with curvature based velocities[10-22]. Those moving curves or surfaces are represented by the level set of a higher dimensional hypersurface. This method provides not only more accurate numerical implementations, but also can handle topological changes automatically.

In this paper, we'll discuss the drawbacks in previous geometric active contour models, and present a new geometric active contour model. This model can overcome some problems with previous models. We implement the level set algorithm to solve the new geometric active contour model. The efficacy of the proposed model in this paper is demonstrated with numerical experiments on synthetic images and medical images.

2 Background and Related Work

Based on the theory of the curve evolution, Caselles et al.[2] and Malladi et al.[3,16] proposed the geometric active contour models independently. In these active contour models, the curve or surface is propagating by means of a velocity which is a function of the curvature. This velocity function usually contains two terms, one is related to the regularity of the curve and the other shrinks or expands the curve towards the boundaries. In order to stop the curve propagating on the edges, a function of the image features of interest is multiplied to the velocity function. The models are as follows:

$$\frac{\partial C(p,t)}{\partial t} = g(I)(\nu + \kappa)\vec{\mathcal{N}}^{[2]} \tag{1}$$

or

$$\frac{\partial C(p,t)}{\partial t} = g(I)(1 - \epsilon\kappa)\vec{\mathcal{N}}^{[3,16]} \tag{2}$$

where C(p,t) denotes the closed evolving contour, $\nu \geq 0$, $\epsilon > 0$ constants, κ is the curvature, $\vec{\mathcal{N}}$ is the unit normal vector(inward or outward) along the evolving contour.

$$g(I) = \frac{1}{1 + \|\nabla G_\sigma * I\|^m}, \quad m = 1 \text{ or } 2 \tag{3}$$

G_σ is a Gaussian filter or any other smooth filters, σ is the scale-space parameter. ∇ is the gradient operator.

Kichenassamy et al.[17-18] derived another geometric active contour model, geodesic active contour model, from the curve shortening theory and the conformal Eulidean metric on $\mathcal{R}^2$ as follows:

$$\frac{\partial C(p,t)}{\partial t} = g(I)(\nu + \kappa)\vec{\mathcal{N}} - (\nabla g \cdot \vec{\mathcal{N}})\vec{\mathcal{N}} \tag{4}$$

0-8186-8821-1/98 $10.00

Caselles et al.[19−20] also obtained the model above by unifying the curve evolution approaches with the classical energy minimization method.

These geometric active contour models have the significant advantage over classical snakes that changes in topology due to the splitting and merging of multiple contours, are handled in a natural way when implemented using the level set based numerical algorithm[7−9]. But there are also some problems associated with these models. First, an important issue of these models is the selection of the stoping function g(I).

In [16], assuming curve moving with speed $F(\kappa) = F_A + F_G$, the term F_A, referred to as the advection term, is independent of the moving contour's geometry, F_G is the part which depends on the geometry of the moving contour such as its local curvature κ. If F_G=0, [16] defined a new speed function $F(\kappa) = F_A + \hat{F}_I$, where

$$\hat{F}_I = \frac{-F_A}{M_1 - M_2}\{\|\nabla G_\sigma * I\| - M_2\} \qquad (5)$$

M_1 and M_2 are the maximum and minimum values of the magnitude of the smoothed image gradient $\|\nabla G_\sigma * I\|$, this new speed function doesn't work for the image whose gradients suffer from large variations, since $(F_A + \hat{F}_I)$ ranges between F_A and zero, only when $\|\nabla G_\sigma * I\|$ approaches the maximum M_1 at the object boundaries, the new speed function attains zero, otherwise, the new speed is always greater than zero. If $F_G \neq 0$, [16] didn't find an additive speed term from the image that will cause the net speed of the moving contour to approach zero in the neighborhood of a desired shape. Instead, they multiply the speed function $F(\kappa) = F_A + F_G$ with g(I):

$$g(I) = \frac{1}{1 + \|\nabla G_\sigma * I\|}, \quad or \quad g(I) = e^{-\|\nabla G_\sigma * I\|} \qquad (6)$$

However, in some cases, if the initial contour is much closer to one portion of the object boundaries than another, the evolving contour crosses over object boundaries closest to it since the stop function is small, but not zero, near and at the boundaries[21].

In model (4), an extra stopping term $\nabla g \cdot \vec{\mathcal{N}}$ introduced. They called this term like a "doublet" near an edge[17−18], and claimed this extra term attracts the evolving contour to the boundaries of the objects as the evolving contour approaches the boundaries[17−20]. Actually, since $(\nu + \kappa)$ and $\nabla g \cdot \vec{\mathcal{N}}$ depend on the shape of the evolving contour, it is very difficult to choose g(I) and ν such that $(g(I)(\nu + \kappa) - \nabla g \cdot \vec{\mathcal{N}})$ is zero for all points on the evolving contour when they move to the boundaries. In fact, for step edges, $(g(I)(\nu+\kappa) - \nabla g \cdot \vec{\mathcal{N}})$ can not be zero anywhere, since on the homogeneous region, $g(I) \approx 1$, $\nabla g \approx 0$, therefore $g(I)(\nu+\kappa) - \nabla g \cdot \vec{\mathcal{N}} \approx \nu + \kappa > 0$, but on the edges, $g(I) \approx 0$, $\|\nabla g\| > 0$, therefore $g(I)(\nu + \kappa) - \nabla g \cdot \vec{\mathcal{N}} \approx -\nabla g \cdot \vec{\mathcal{N}} < 0$. In addition, for the contour points which $(g(I)(\nu + \kappa) - \nabla g \cdot \vec{\mathcal{N}}) > 0$, those points will pass over the edges, for the contour points which $(g(I)(\nu + \kappa) - \nabla g \cdot \vec{\mathcal{N}}) < 0$, those points will move in reversed direction along the normal vector back to the interest region, then move to the edges again after g(I) getting larger and $\|\nabla g\|$ getting smaller such that $(g(I)(\nu + \kappa) - \nabla g \cdot \vec{\mathcal{N}}) > 0$. Thus, the contour points may fluctuate near the edges. Therefore, the evolving contour is stable on the boundaries finally not because the evolving speed is zero, instead, all points on the evolving contour achieve a dynamic balance. That means that the evolving speed will change the sign such that the points on the evolving contour move back and forth near boundaries unless they move in very small distance comparing to one pixel. Sometime, this may take a long time to reach balance. On the other hand, model (4) can not detect the ramp edges well, or may be captured by weak or spurious edges if $(g(I)(\nu+\kappa) - \nabla g \cdot \vec{\mathcal{N}}) \leq 0$ on these edge points. Obviously, it depends on the choice of g(I) and ν, accordingly, ν may have influence on edge detection.

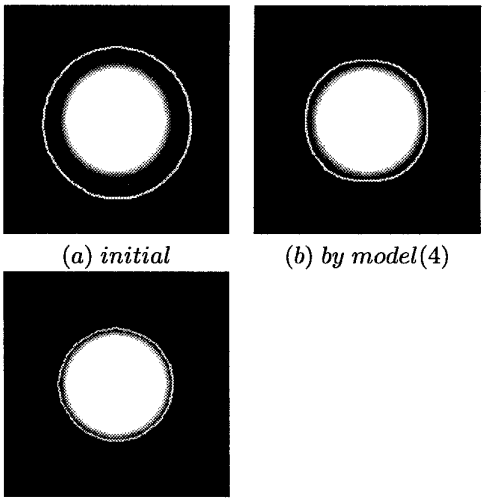

(a) *initial* (b) *by model*(4)

(c) *by model*(12)

Figure 1: Ramp edges detection by model(4) and model(12).

Figure 1 shows (a) a synthetic image which consists

of a disk of intensity 100 on a background of intensity zero, with a blur filter applied to it. The blur filter is a normalized $k \times k$ box filter with unity entries. (b) the segmentation result applying model (4) for k=7, $\nu = 1$. After 16 iterations, the evolving contour stops changing, and is stable there.

From figure 1, we can find the evolving contour is captured by weak edges.

In addition, model (1), (2), and (4) are kind of multiplication models, the product of speed and stoping function under small speed or small stoping function may be same, but they have very different physical meanings.

3 New Geometric Active Contour Model

In this section, we'll present a new geometric active contour model—addition model.

Let $C(p,t) = (x(p,t), y(p,t))^T$ be a family of parameterized planar curves in $\mathcal{R}^2$ which is generated by moving an initial contour. Where p parameterizes the curves, t parameterizes the family(t usually time).

The evolution equation of this family of curves describing the differential change of the curves in t can be written as[23]

$$\begin{cases} \dfrac{\partial C(p,t)}{\partial t} &= < \vec{\mathbf{v}}, \vec{\mathcal{N}} > \vec{\mathcal{N}} + < \vec{\mathbf{v}}, \vec{\mathcal{T}} > \vec{\mathcal{T}} \\ C(p,0) &= C_0(p) \end{cases} \quad (7)$$

Where $\vec{\mathbf{v}}(p,t)$ is the velocity vector of the curves evolving at point (p,t). $\vec{\mathcal{N}}$ and $\vec{\mathcal{T}}$ are the unit normal vector and unit tangent vector respectively. $< \cdot, \cdot >$ denotes the Euclidean inner product. $< \vec{\mathbf{v}}, \vec{\mathcal{N}} >$ and $< \vec{\mathbf{v}}, \vec{\mathcal{T}} >$ are the normal and tangent components of the evolution velocity $\vec{\mathbf{v}}(p,t)$ respectively.

A basic result from the theory of the curve evolution is that the geometric shape of the curve is only affected by the normal component of the velocity, the tangential component of the velocity affects only the parameterization of the curves, not the geometric shape of the curves[24].

Therefore, (7) can be written as

$$\begin{cases} \dfrac{\partial C(p,t)}{\partial t} &= < \vec{\mathbf{v}}, \vec{\mathcal{N}} > \vec{\mathcal{N}} \\ C(p,0) &= C_0(p) \end{cases} \quad (8)$$

This means curve evolution is determined by its normal component of the velocity. Now, the question is how to choose a velocity function such that the curve evolves to the boundaries of the interest objects.

Let's decompose the normal component of the velocity into two components as follows:

$$< \vec{\mathbf{v}}, \vec{\mathcal{N}} >= v_{int} + v_{ext}$$

where v_{int} is the velocity component along the normal direction from the curve itself to move the curves outward or inward and keep the curves smooth. v_{ext} is the velocity component along the normal direction computed from image data which is in the reversed direction as $v_{int}\vec{\mathcal{N}}$ to stop the evolving curves at the boundaries.

since constant speed will often lead to singularities in shape, while curvature speed will smooth shapes[4–6]. Sketches of these principles are shown in figure 2[9].

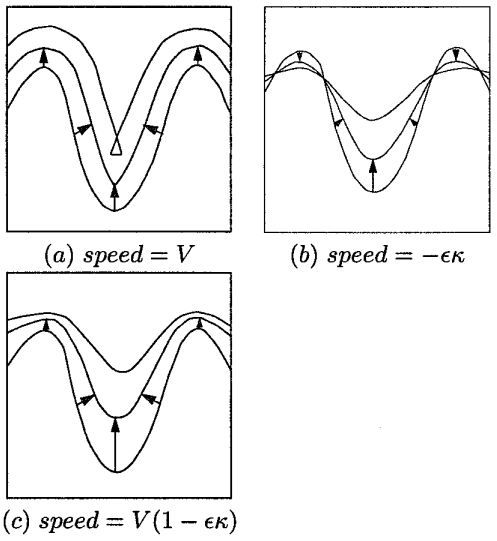

(a) $speed = V$ (b) $speed = -\epsilon\kappa$

(c) $speed = V(1 - \epsilon\kappa)$

Figure 2: Speed dependent on curvature. Here $\kappa > 0$ for convex shape, and $\kappa < 0$ for concave shape .

Therefore, we take

$$v_{int} = f(\kappa) \quad (9)$$

a function of curvature.

In order to make the evolving curves stop at the boundaries, we can take

$$v_{ext} = -\gamma f(\kappa) P(I) \quad (10)$$

where

$$P(I) = \begin{cases} 1 & if \ \|\nabla G_\sigma * I\| > T_0 \\ 0 & \text{otherwise} \end{cases} \quad (11)$$

$\gamma \geq 1$, a constant, such that edge points can stop the evolving contour. T_0 is a threshold value.

Thus, (8) can be written as

$$\frac{\partial C(p,t)}{\partial t} = (1 - \gamma P(I)) f(\kappa) \vec{\mathcal{N}} \quad (12)$$

In order to compute the evolution of the equation (12), using level set method, this can be converted to evolve the embedding function u(x, y, t) according to[7–9]:

$$\frac{\partial u}{\partial t} = (1 - \gamma P(I)) f(\kappa) \|\nabla u\| \qquad (13)$$

Model (12) and (13) are same for 2D and 3D images.

4 Experimental Results

In this section, we'll apply the narrow band level set algorithm[16,25–26] to solve the model (13) for segmentation.

Figure 1(c) shows the segmentation result by $f(\kappa) = 1 - 0.05\kappa, \gamma = 1$ in model(12), k=7, $T_0 = 100$. After 18 iterations, the evolving contour stop moving. Here, we found the right boundaries were detected by the new geometric active contour model in section III.

Figure 3 shows a synthetic image E with intensity 255 on E and zero intensity on the background. This image is degraded by noise , SNR=10 dB. the initial contour and the segmentation results are shown in figure 3 too. $f(\kappa) = 1, \gamma = 1 + 2 \times 10^{-5}$.

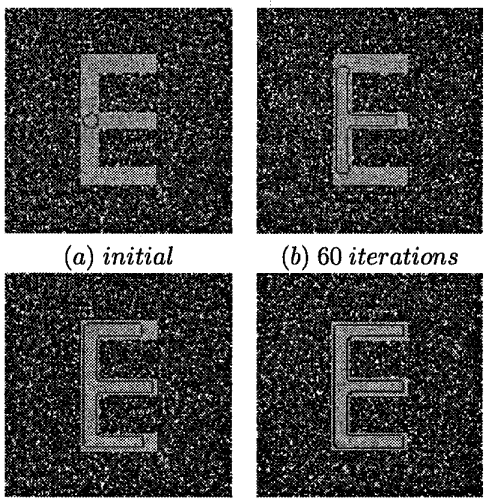

(a) *initial* (b) 60 *iterations*

(c) 120 *iterations* (d) 154 *iterations*

Figure 3: The synthetic image E degraded by noise, SNR=10 dB, and the segmentation results using proposed model.

Figure 4 depicts the segmentation of the MR heart ventricle images. In figure 4, $f(\kappa) = 1 - 0.05\kappa, \gamma = 1 + 2 \times 10^{-5}$, (a) shows the initial contour which envelops the left and right ventricles, (b)-(c) show evolution of the evolving contour at 50th, 93th respectively, and (d) shows the final result. The evolving contour splits automatically at the 94th iteration.

In all experiments above, we took $\gamma = 1 + \delta, \delta = 0$ or $\delta = 2 \times 10^{-5}$, a very small number, this can relieve or eliminate the fluctuations when the moving contour approaches the edges, since very small speed $-\delta f(\kappa)$ can only move the points on the evolving contour less than 0.2(say) pixels, this means the points on the evolving contour don't move back to the interior of the interest region actually.

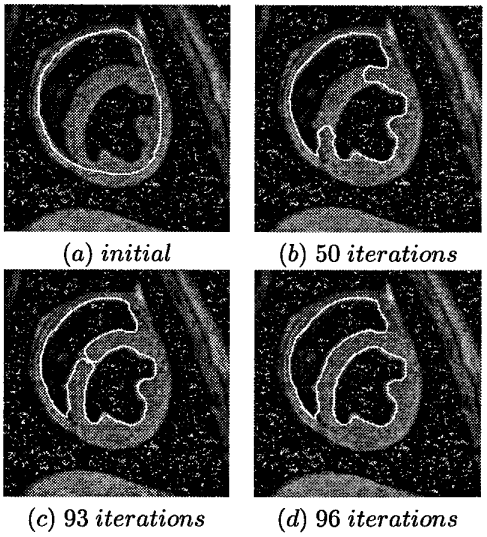

(a) *initial* (b) 50 *iterations*

(c) 93 *iterations* (d) 96 *iterations*

Figure 4: The heart ventricles and the segmentation results using proposed model.

5 Conclusions

In this paper, we have presented a new geometric active contour model. This model can overcome some problems associated with the previous models. We use level set method to solve PDEs. This model has been applied to segment synthetic and MR images, the experimental results indicated the efficacy of the proposed scheme.

References

[1] M. Kass, A. Witkin, and D. Terzopoulos, "Snakes: active contour medels", *Int. J. Computer Vision*, Vol. 1, pp. 321-331, 1988.

[2] V. Caselles, F. Catte, T. Coll, and F. Dibos, "A geometric model for active contours in image processing," *Numerische Mathematik*, Vol. 66, pp. 1-31, 1993.

[3] R. Malladi, J.A. Sethian, and B.C. Vemuri, "Evolutionary fronts for topology-independent shape modelling and recovery," in *Proc. 3rd ECCV, LNCS-800*, Stockholm, Sweden, pp. 3-13, May 1994.

[4] M. Gage and R. S. Hamilton, "The heat equation shrinking convex plane curves," *J. Differ. Geom.*, Vol. 23, pp. 69-96, 1986.

[5] M.A. Grayson, "The heat equation shrinks embedded plane curves to round points," *J. Differ. Geom.*, Vol. 26, pp. 285-314, 1987.

[6] M.A. Grayson, "Shortening embedded curves," *Annals of Mathematics*, Vol. 129, pp. 71-111, 1989.

[7] J.A. Sethian, "Curvature and the evolution front," *Comm. Math. Phys.*, Vol. 101, pp. 487-499, 1985.

[8] S. Osher and J.A. Sethian, "Fronts propagating with vurvature-dependent speed: algorithms based on Hamilton-Jacobi formulations," *J. comput. phys.*, Vol. 79, pp. 12-49, 1988.

[9] J.A. Sethian, "Numerical algorithms for propagating interfaces: Hamilton-Jacob equations and conservation laws," *J. Diff. Geom.*, Vol. 31, pp. 131-161, 1990.

[10] B.B. Kimia, A. Tannenbaum, and S.W. Zucker, "Toward a computational theory of shape: an overview," *LNCS-427*, pp.402-407, Springer, New York, 1990.

[11] B.B. Kimia, A. Tannenbaum, and S.W. Zucker, "Shapes, shocks, and deformations I: the components of two-dimensional shape and the reaction-diffusion space," *Int. J. computer vision*, Vol. 15, pp. 189-224, 1995.

[12] G. Sapiro, R. Kimmel, D. Shared, B.B. Kimia and A.M. Bruckstein, "Implementing continuous-scale morphology via curve evolution," *Pattern Recognition*, Vol. 26, pp. 1363-1372, 1993.

[13] G. Sapiro and A. Tannenbaum, "Affine invariant scale-space," *Int. J. Computer vision*, Vol. 11, pp. 25-44, 1993.

[14] G. Sapiro and A. Tannenbaum, "On affine plane curve evolution," *J. Functional Analysis*, Vol. 119, pp. 79-120, 1994.

[15] G. Sapiro and A. Tannenbaum, "Area and length preserving geometric invariant scale-space," *IEEE Trans. on PAMI*, Vol. 17, pp. 67-72, 1995.

[16] R. Malladi, J.A. Sethian, and B.C. Vemuri, "Shape modelling with front propagation: a level set approach," *IEEE Trans. on PAMI*, Vol. 17, pp. 158-175, 1995.

[17] S. Kichenassamy, A. Kumar, P. Olver, A. Tannenbaum, and A. Yezzi, "Gradient flows and geometric active contours," in *Proc. ICCV'95*, Cambriadge, June 1995.

[18] S. Kichenassamy, A. Kumar, P. Olver, A. Tannenbaum, and A. Yezzi, "Conformal curvature flows: from phase transitions to active vision," *Arch. Rational Mech. Anal.*, Vol. 134, pp. 275-301, 1996.

[19] V. Caselles, R. Kimmel, G. Sapiro, "Geodesic active contours," *Int. J. computer vision*, Vol. 22, pp. 61-79, 1997.

[20] V. Caselles, R. Kimmel, G. Sapiro and C. Sbert, "Minimal surfaces based object segmentation," *IEEE Trans. on PAMI*, Vol. 19, pp. 394-398, 1997.

[21] H. Tek and B.B. Kimia, "Volumetric segmentation of medical images by three-dimensional bubbles," *CVIU*, Vol. 65, pp. 246-258, 1997.

[22] R. Kimmel, A. Amir, A.M. Bruckstein, "Finding shortest paths on surfaces using level sets propagation," *IEEE Trans. on PAMI*, Vol. 17, pp. 635-640, 1995.

[23] M.P. Do Carmo, *Differential geometry of curves and surfaces,* Prentice-Hall, Englewood Cliffs, New Jersey, 1976.

[24] C.L. Epstein and M. Gage, *The curve shortening flow, wave motion: theory, modeling, and computation,* A. Chorin and A. Majda(Eds), Springer, New York, 1987.

[25] D. Chopp, "Computing minimal surfaces via level set curvature flow," *J. Comput. Phys.* Vol. 106, pp. 77-91, 1993.

[26] D. Adalsteinsson and J.A. Sethian, "A fast level set method for propagating interfaces," *J. Comput. Phys.*, Vol. 118, pp. 269-277, 1995.